Ultrasonics 116 (2021) 106496

Contents lists available at ScienceDirect

Ultrasonics

journal homepage: www.elsevier.com/locate/ultras

New modification of the acoustic Lamb waves and its application for liquid and ice sensing

V.I. Anisimkin [a], N.V. Voronova [b]

[a] Kotel'nikov Institute of Radio Engineering and Electronics of RAS, Moscow, Russia
[b] Acoustoelectronic and Piezokeramic ELPA Corporation Moscow, Russia

ARTICLE INFO

Keywords:
Crystal plate
Lamb wave
Elastic displacement
Depth profile
Liquid
Ice
Viscosity
Attenuation

ABSTRACT

Using quartz plates as an example existance of the new modification of the Lamb waves is demonstrated. The waves have small vertical displacement, large shear-horizontal and longitudinal components, and elliptic polarization which is oriented parallel to the plate faces. Numerical calculations of the surface displacements and depth profiles show the particular polarization is maintained at any depth from free faces and for all plate thickness in the range $h/\lambda = 0$–1.7 (h - thickness, λ - wave length). Results of the measurements accomplished for four new modes and three plate thickness h/λ confirm that radiation of the waves into adjucent liquid (which is proportional to vertical displacement) is small, while viscoelestic loss of the same the waves (which is proportional to in-plane components) is large. This property makes the modified waves suitable for sensing liquids and ices. In particular, responses of the waves towards liquid viscosity and water-to-ice transformation are larger than those are for common Lamb waves approaching 27 and 50 dB, respectively, at about 30 MHz, 1500 cP, and 10 mm propagation path.

1. Introduction

The spectrum of the acoustic waves in crystal plates is very manifold and variable (Fig. 1) [1–16]. It includes three families of waves with different polarizations - shear-horizontal (SH), quasi-longitudinal (Anisimkin Jr., AN), and three- or two-partial Lamb waves. The 1st family has only one u_2 displacement component (Fig. 1). It may exist only in some crystals of special orientations [1]. The 2nd family has dominant longitudinal displacement component u_1 [4,6,7] (Fig. 1). It exists almost in all crystals and orientations, but only for allowable plate thickness separated by forbidden "bands". The waves of this type propagate with velocities v_n close to the velocity of the longitudinal bulk wave v_L, travelling in the same direction. Instead, the generalized Lamb waves (the most popular acoustic plate waves) have three displacement components - longitudinal u_1, shear-horizontal u_2, and shear-vertical u_3. Depending on the amplitudes and phases of the components the total polarization of the waves may have four different forms: i) elliptic with plane of the ellipse parallel to X_3-k (sagittal) plane, ii) elliptic with the ellipse inclined to that plane, iii) elliptic with the ellipse rotated around the plate normal X_3, and iv) elliptic with the ellipse both inclined and rotated (as shown on Fig. 1). At special conditions some Lamb waves may radiate energy in opposite direction [15,16].

All these properties allow use acoustic plate waves for filters, resonators, sensors, and liquid-to-ice analysis [5,9,11,12,17–21]. Taking into account modern state of art in solid state acoustics it could be expected that all applications may be essentially improved through exploiting other waves with better properties.

The goal of the present paper is to show that i) the Lamb waves in crystal plates may have elliptic polarization which is oriented parallel to the plate faces ($u_3 \ll u_1$, $u_2 \neq 0$) (Fig. 2) and ii) the modified waves are useful for sensing liquid viscosity and ice formation.

L, longitudinal or Anisimkin Jr.'; SH, shear horizontal; Lamb, two- or three-component (elliptic); k, propagation direction (x_1 axis); u_1, u_2, u_3, partial displacements; h, plate thickness; x_3, plate normal.

2. Strategy

Numerical calculations are accomplished for quartz plates of the ST, X-cut with Eugler angles 0°, 132.75°, 0°, as an example. The normalized thickness of the plate h/λ is varied from 0 to 1.7 in order to provide most essential difference between modes of different orders n. Dispersion curves $v_n(h/\lambda)$, surface displacements u_1^0, u_2^0, u_3^0, and depth profiles $u_1(x_3/\lambda)$, $u_2(x_3/\lambda)$, $u_3(x_3/\lambda)$ are numerically calculated, using PC software from McGill University [22] and material constants from [23].

E-mail address: anis@cplire.ru (V.I. Anisimkin).

https://doi.org/10.1016/j.ultras.2021.106496
Received 15 April 2021; Received in revised form 30 May 2021; Accepted 3 June 2021
Available online 7 June 2021

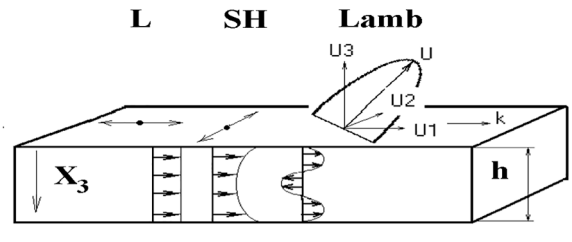

Fig. 1. Schematic of the acoustic plate waves known so far.

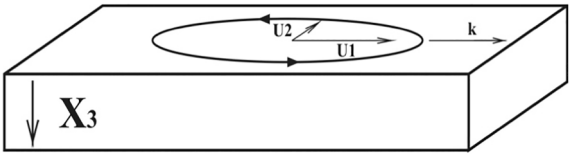

Fig. 2. Schematic of the new modification of the Lamb waves with negligible vertical displacement u_3 ($u_3 \ll u_1$, $u_2 \neq 0$) and elliptic polarization oriented parallel to the plate faces.

Procedure of the calculations is as follows. First, velocities v_n and surface displacements u_1^0, u_2^0, u_3^0 of all modes at a fixed plate thickness $h/\lambda = 1.0$ are calculated. Then, the modes with negligible shear-vertical displacement on the surface ($u_3^0 \ll u_1^0$, $u_2^0 \neq 0$) are selected and the surface displacements $u_1^0(h/\lambda)$, $u_2^0(h/\lambda)$, $u_3^0(h/\lambda)$, $v_n(h/\lambda)$ are calculated for the modes and other plate thickness h/λ in the range 0 – 1.7. This step allows clarify how the properties of the selected modes depend on h/λ.

After that, the depth profiles $u_1(x_3/\lambda)$, $u_2(x_3/\lambda)$, and $u_3(x_3/\lambda)$ are calculated for some selected modes and various plate thickness $h/\lambda = 0.44$, 1.0, and 1.5. This step allows clarify, whether elliptic polarization of the modes is maintained for different depths from free faces.

Finally, existance of the new waves is qualitatively verified experimentally using four new modes and three plate thickness $h/\lambda = 0.6$, 1.0, and 1.67 ($h = 300$ and 500 μm, $\lambda = 200$ and 300 μm). Quartz plate has one grinded (top) and one polished (bottom) surface. The top surface is used for liquid deposition on the propagation path. The bottom surface contains two interdigital transducers (IDTs) comprised of 20 or 50 finger electrodes (1000-nm-thick Cr/Al). The bandwidth of the transducers (5 or 2%) provides good frequency resolution of the neighbor modes. Precision of the velocity measurements is about ± 1 or 0.5%.

The measurements with viscous liquid (glycerin) are accomplished as follows [24]. First, for each mode n the value of the insertion loss S_{12}^{air} is measured in air (without liquid) at relevant frequency $f_n = v_n/\lambda$ (v_n – the mode velocity, λ - the wavelength and the period of the transducers). Second, the same loss S_{12}^{H2O} and $S_{12}^{Glycerin}$ are recorded after distilled water (viscosity $\eta = 1.003$ cP, 600 mg) or pure glycerin ($\eta = 1\,490$ cP, 600 mg) are deposited by syringe on the propagation path on the top surface. The new modes are identified as those having i) relevant velocity v_n together with ii) small radiation loss S_{12}^{H2O} - S_{12}^{air} (proportional to u_3^0) and iii) large viscoelastic loss $S_{12}^{Glycerin}$ - $S_{12}{}^{H2O}$ (proportional to u_1^0 and u_2^0). Responses of the modes towards viscosity η are defined as $\Delta S_{12} = S_{12}{}^{Glycerin}$ - $S_{12}{}^{H2O}$.

The ice measurements are performed in climatic room (UC-20CE, 20 L in volume) whose temperature is varied from + 20 to −15 °C for 1100 sec and controlled by iron-constantan thermocouple. Here, for each mode n the loss S_{12}^{air} is first measured in air at + 20 °C. Then, the same loss S_{12}^{H2O} is recorded for distilled water (600 mg) at + 20 °C. Finally, quartz plate is cooled and the loss S_{12}^{ice} is measured at −15 °C, when water freezes totally. Responses of the modes towards ice formation are defined as $\Delta S_{12} = S_{12}^{ice}$-$S_{12}{}^{H2O}$.

All measurements are accomplished with KEYSIGHT 5061B network analyser, operating in amplitude-frequency format and GATE option in order to avoid rf leakage [21].

Table 1
Velocities v_n and surface displacements u_1^0, u_2^0, u_3^0 of the Lamb waves in ST,X-quartz plate with normalized thickness $h/\lambda = 1.0$. Bold are the modes with $u_3^0 \ll u_1^0$, u_2^0.

n	v_n(calculated)/v_n(measured)*, m/s	u_1^0/u_1^0	u_2^0/u_1^0	u_3^0/u_1^0
0	2912/2910 ± 30	1	0.15	1.6
1	4205/4170 ± 40	1	0.11	1.3
2	5029/5040 ± 50	1	2.2	0.34
3	5366/5370	1	3.7	0.16
4	5751/5790 ± 60	1	0.066	0.086
5	6038	1	0.57	0.18
6	**6385**	**1**	**1.6**	**0.029**
7	6850/6840 ± 70	1	0.51	0.5
8	6911	1	0.31	0.79
9	**7744/7770 ± 80**	**1**	**1.9**	**0.15**
10	8279/8280 ± 80	1	1.1	2.5
11	**8724/8700 ± 90 (MODE 1)**	**1**	**0.4**	**0.12**
12	9326/9300 ± 90	1	1.9	0.35
13	**10231/10230 ± 100**	**1**	**0.48**	**0.11**
14	10,753	1	0.95	1
15	11199/11220 ± 110	1	25	22
16	11,851	1	0.53	0.57
17	**12,637**	**1**	**0.92**	**0.15**
18	13239/13200 ± 130	1	1.1	0.23
19	**14372/13500 ± 140 (MODE 4)**	**1**	**0.63**	**0.0018**
20	14,529	1	9.2	130
21	**14,957 (MODE 2)/14920 ± 150**	**1**	**1.6**	**0.007**
22	16,083	1	0.4	0.14
23	**16732/16710 ± 150**	**1**	**2.6**	**0.12**
24	17,539	1	0.2	0.64
25	18,087	1	0.12	1.7
26	18,568	1	4.3	0.44
27	**19,330**	**1**	**0.14**	**0.081**
28	**20,434**	**1**	**8.7**	**0.057**
29	**21,001 (MODE 3)**	**1**	**0.082**	**0.016**
30	21,373	1	0.072	14
31	22,329	1	18	0.29
32	22,678	1	0.042	0.13
33	24,238	1	96	18
34	24,903	1	0.053	3.7
35	25,962	1	0.02	0.043

* Modes with too closed velocities $\Delta v_n/v_n < 2\%$ interfere with each other making rigorous measurements impossible. Modes with too small coupling constants $k_n^2 < 0.01\%$ are not detected because of too large insertion loss.

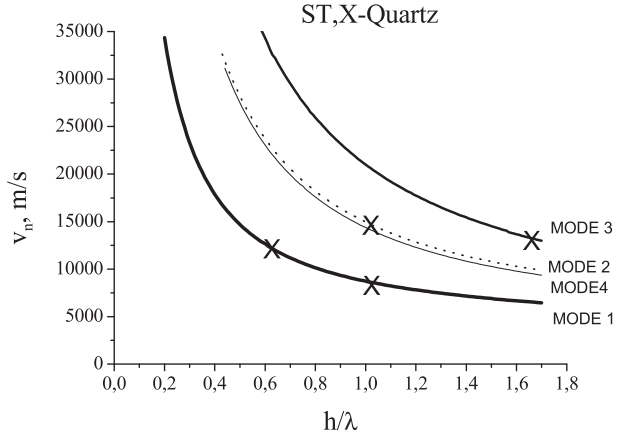

Fig. 3. Dispersion curves of the modified Lamb waves with displacement ellipse parallel to the plate faces. Plate: ST,X-quartz with free faces. Curves – numerical calculations; x – examples for detailed analysis.

3. Results and discussion

Results of the calculations are presented in Table 1 and Figs. 3-7.

Table 1 shows first 36 acoustic waves existing in ST,X-quartz plate with normalized thickness $h/\lambda = 1.0$. The measured velocities of the

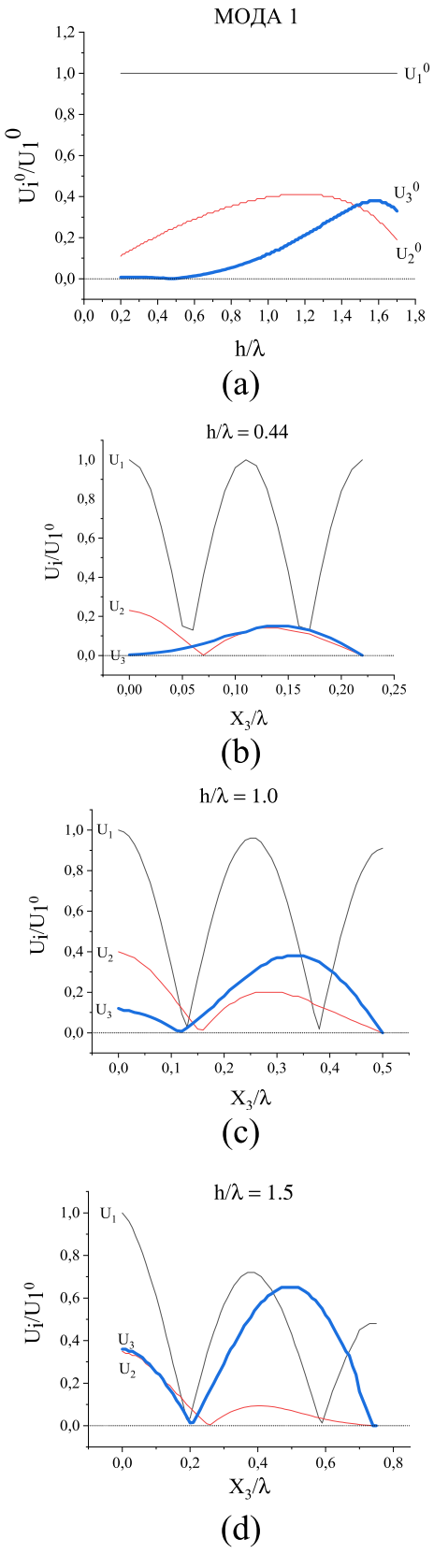

Fig. 4. Surface displacements (a) and depth profiles (b-d) of the modified Lamb MODE 1 depicted in Table 1 as bold.

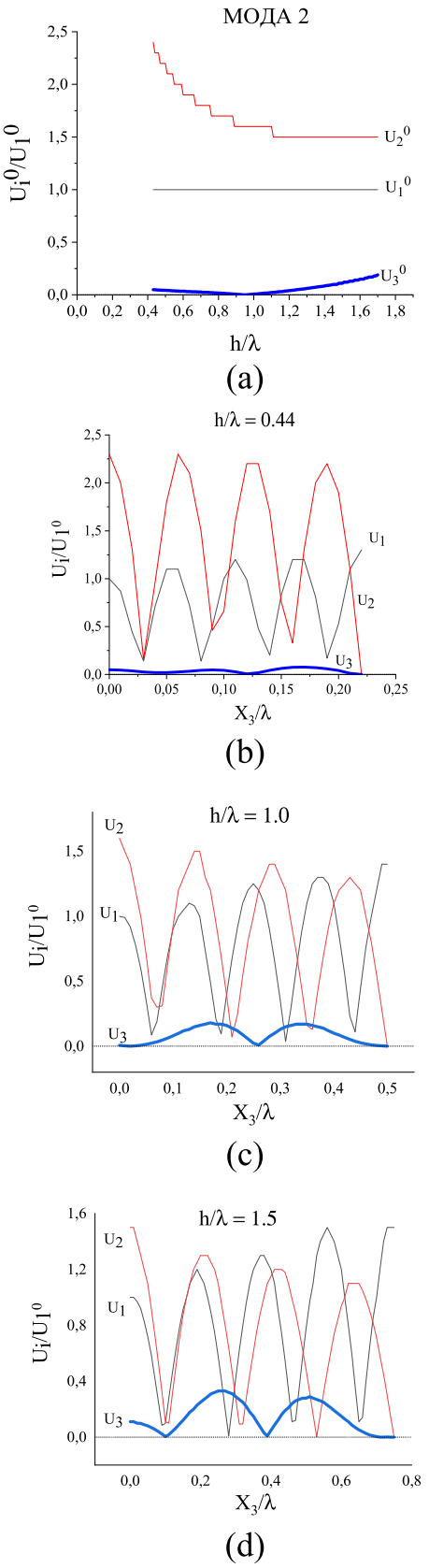

Fig. 5. Surface displacements (a) and depth profiles (b-d) of the modified Lamb MODE 2 depicted in Table 1 as bold.

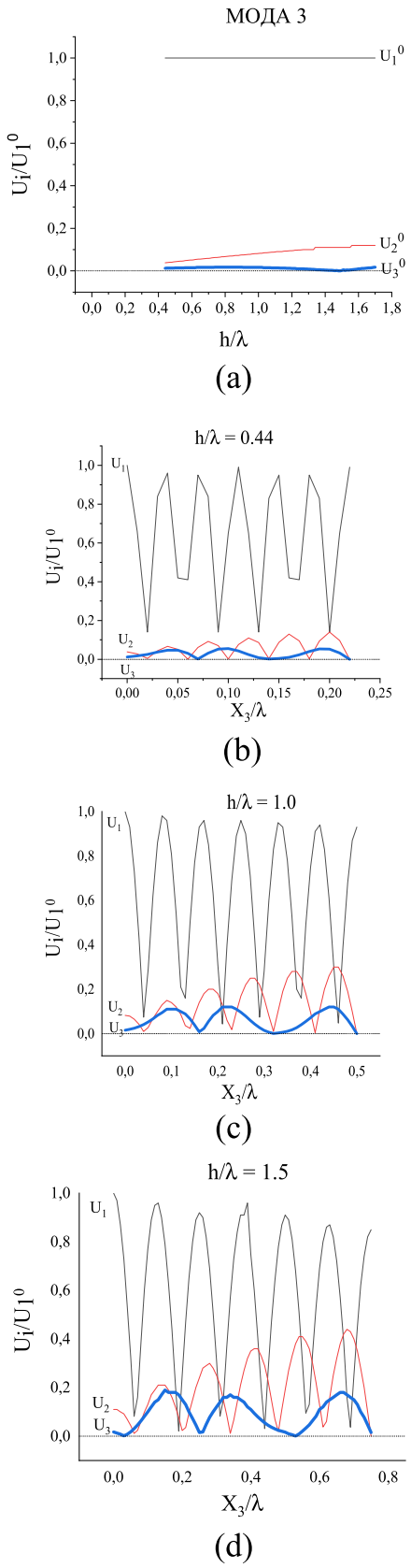

Fig. 6. Surface displacements (a) and depth profiles (b-d) of the modified Lamb MODE 3 depicted in Table 1 as bold.

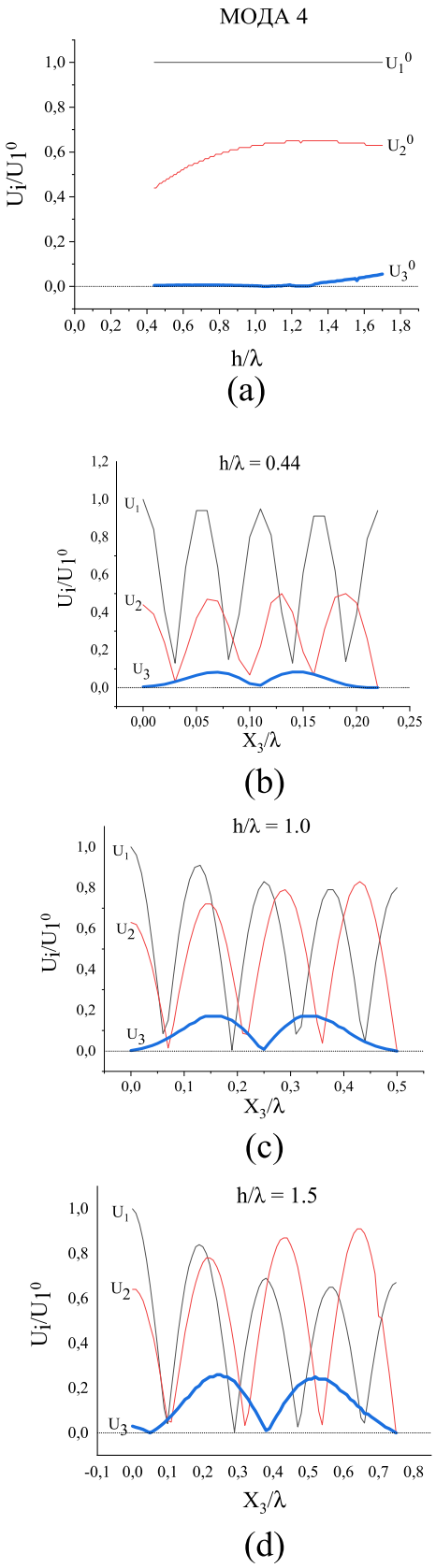

Fig. 7. Surface displacements (a) and depth profiles (b-d) of the modified Lamb MODE 4 depicted in Table 1 as bold.

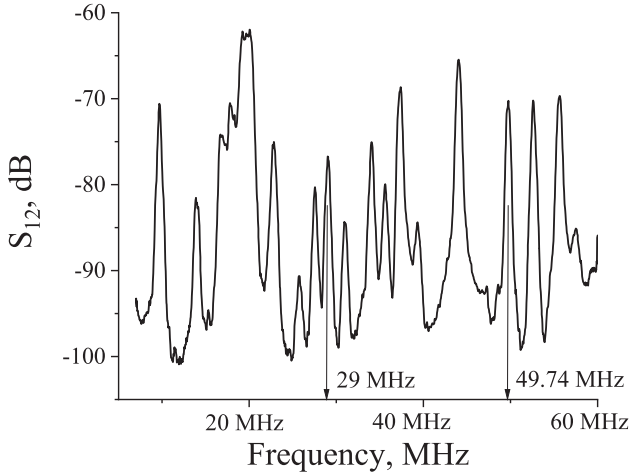

Fig. 8. Insertion loss (transfer function) S_{21} of the delay line implemented on ST,X-quartz plate with normalized thickness $h/\lambda = 1.0$ as measured by network analyzer in air at 20 °C. Frequencies of the Lamb waves with small vertical displacement u_3^0 and elliptic polarization oriented parallel to the plate faces are indicated by arrows.

waves are in agreement with calculations.

Analysis of the wave displacements shows that acoustic spectrum of the plate modes is very manifold even for a given crystal, orientation, plate thickness, and propagation direction (Table 1). Most waves (n = 0, 1, 7, 8, 10, 14, 16, 24, 25, 30, 32, 34) belong to the Lamb family [1] as they have comparable longitudinal u_1^0, shear-horizontal u_2^0, and shear-vertical u_3^0 displacements (three-partial waves) or small u_2^0 and comparable u_1^0 and u_3^0 components (two-partial waves).

The mode n = 4 is quasi-longitudinal [4,6,7] as $u_1^0 \gg u_2^0, u_3^0$. Polarization of the mode is parallel to the propagation direction, and the mode velocity v_n (5751 m/s) is close to the velocity of the longitudinal bulk wave, travelling in the same direction (v_L = 5744 m/s).

The modes n = 31 and 33 are almost shear-horizontal waves ($u_2^0 \gg u_1^0, u_3^0$).

The mode n = 20 is almost a shear-vertical wave ($u_3^0 \gg u_1^0, u_2^0$).

At the same time, Table 1 contains large group of modes (bold) whose elastic polarization is modified in such a way that vertical displacement on the plate faces u_3^0 is very small as compared with other two components ($u_3^0 \ll u_1^0, u_2^0$) shifted towards each other on about π/2. As a result, polarization of the modes is elliptic with plane of the ellipse oriented parallel to the plate faces. In ST,X-quartz the number of modes possessing this property is 11. Four of them (MODES 1–4, Table 1) are taken for further investigation vs depth of the plate x3/λ and plate thickness h/λ (Figs. 3-7).

Fig. 3 shows dispersion curves of the selected modes with modified polarization. The curves have common shape of monotonic functions decaying with plate thickness h/λ without any flat sections and/or mutual crossing.

The surface displacements of the modes satisfy ration $u_3^0 \ll u_1^0, u_2^0$ for any plate thickness h/λ (Fig. 4a, 5a, 6a, 7a) except h/λ > 1.4 for MODE 1 (Fig. 4a), where $u_2^0 < u_3^0 \ll u_1^0$. For each mode the form of the surface ellipse is varied with h/λ. For each h/λ the surface ellipse is varied with mode order n. For example, MODE 2 has dominant surface displacement u_2^0 along shear-horizontal direction. Therefore, its surface ellipse is perpendicular to the propagation direction. On the other hand, MODES 1, 3, 4 have dominant longitudinal surface displacements u_1^0. Therefore, the surface ellipses of the modes are oriented along the propagation direction.

Moreover, all displacements of the MODES 1, 2, 3, 4 are varied with depth x_3 from plate faces, as usual. Meanwhile, the ratio $u_3(x_3/\lambda) \ll u_1(x_3/\lambda)$, $u_2(x_3/\lambda)$ is maintained valid for any depth x_3/λ and any plate thickness h/λ (Figs. 4-7, b-d) except MODE 1 at $x_3/\lambda > 0.1$ and $h/\lambda > 1.0$

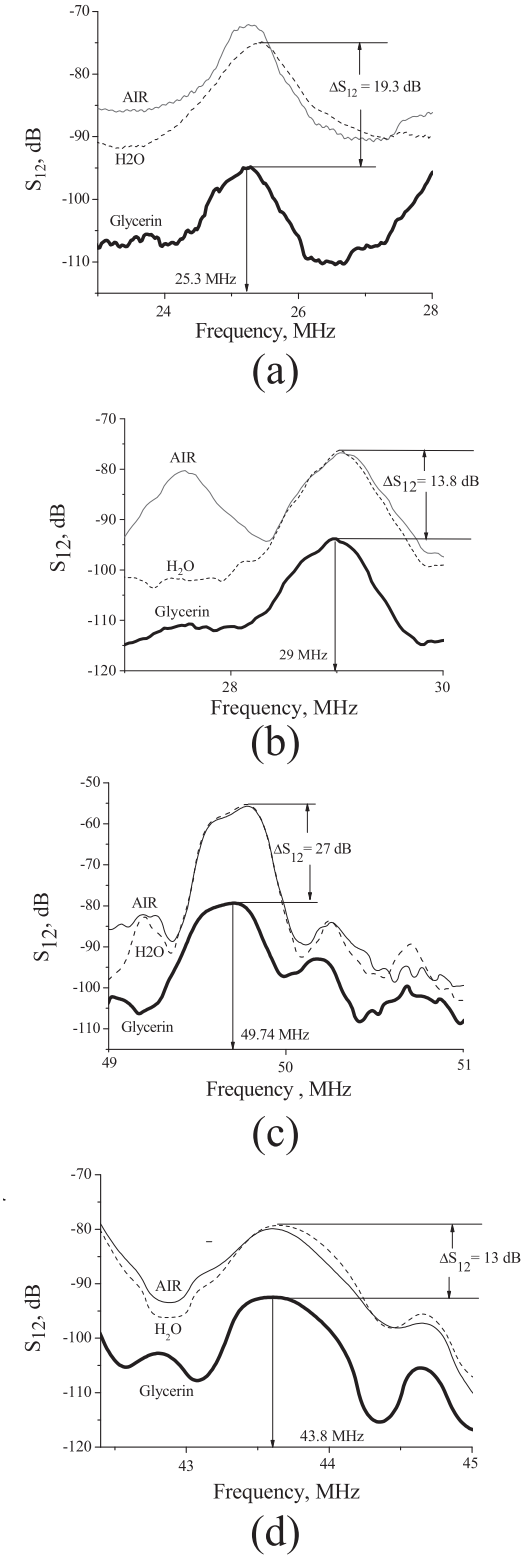

Fig. 9. Insertion loss S_{21} of the modified Lamb modes from Fig. 3 measured for air (solid), water (dashed), and glycerin (bold). (a) – h/λ = 0.9, f_n = 25.3 MHz, v_n = 12 650 m/s (measured) and 12 681 m/s (calculated) m/s, k_n^2 = 0.015%, $\{u_1^0 = 1; u_2^0 = 0.29\ u_1^0; u_3^0 = 0.014\ u_1^0\}$, MODE 1; (b) - h/ λ = 1.0, f_n = 29 MHz, v_n = 8 700 m/s (measured) and 8 724 m/s (calculated), k_n^2 = 0.0082%, $\{u_1 = 1; u_2^0 = 0.4\ u_1^0; u_3^0 = 0.12\ u_1^0\}$, MODE 1; (c) - h/ λ = 1.0, f_n = 49.74 MHz: v_n = 14 920 m/s (measured) and 14 957 m/s (calculated), k_n^2 = 0.0094%, $\{u_1^0 = 1; u_2^0 = 1.6\ u_1^0; u_3^0 = 0.007\ u_1^0\}$, MODE 2; (d) - h/ λ = 1.67, f_n = 43.8 MHz: v_n = 13 140 m/s (measured) and 13180 m/s (calculated|), k_n^2 = 0.003%, $\{u_1^0 = 1; u_2^0 = 0.12\ u_1^0; u_3^0 = 0.014\ u_1^0\}$, MODE 3.

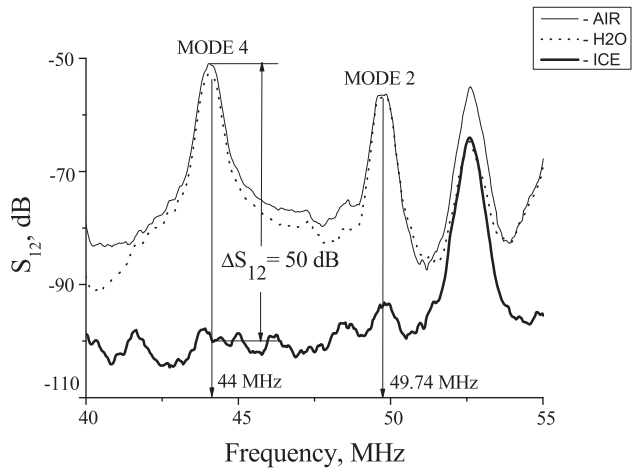

Fig. 10. Insertion loss S_{21} of the MODES 2 and 4 from Fig. 3 measured for air at + 20 °C (thin solid), water at + 20 °C (dotted), and ice at −15 °C (bold). Plate: ST,X-quartz, h = 300 μm, λ = 300 μm, h/λ = 1.0.

(Fig. 4, c, d), where $u_2 < u_3 \ll u_1$. Therefore, almost all displacement ellipses of the new modes are parallel to the plate faces at any depth and for any plate thickness like it is on the surfaces of the plate (Fig. 2).

Zeroing piezoelectric modulii of quartz crystal does not change results of the calculations. However, taking into account small values of the modulii the role of the effect should be studied additionally for more strong piezoelectric materials like $LiNbO_3$ or $LiTaO_3$.

Thus, the new modification of the Lamb waves exists in wide range of propagation conditions, but solely for some waves of the family. Why it is so is not clear yet. The question demands additional investigation.

Fig. 8 shows typical spectrum of acoustic waves detected in crystal plate with free faces. Each mode n of the spectrum is excited in the plate at relevant frequency $f_n = v_n/\lambda$ as it has definite velocity v_n and same wavelength λ defined by period of the transducers. What is most important is that just modes whose velocities close to the velocities of the waves with small vertical displacement u_3^0 possess small radiation loss S_{12}^{H2O} - S_{12}^{air} (proportional to u_3^0) and large viscoelastic loss $S_{12}^{Glycerin}$ - S_{12}^{H2O} (proportional to u_1^0, u_2^0) (Fig. 9). So that because of i) right velocities, ii) small radiation, and iii) large viscoelastic attenuation it is just these modes that may be identified as modified Lamb waves with polarization parallel to the plate faces. Vice versa, other modes detected in the same plate at lower and higher frequencies (Fig. 9, c, d) have different velocities v_n and large radiation loss S_{12}^{H2O} - S_{12}^{air} (Fig. 9, b, c). Therefore, in agreement with calculations they are characterized by large vertical displacements u_3^0 and classified as common Lamb waves.

Responses $\Delta S_{12} = S_{12}^{Glycerin}$ - S_{12}^{H2O} of the modified waves towards liquid viscosity are high. They approach 27 dB (Fig. 9,c). Similarly, responses $\Delta S_{12} = S_{12}^{ice}$ - S_{12}^{H2O} of the same waves towards water-to-ice transformation are also high (50 dB, Fig. 10). They exceed the values measured for common Lamb waves in $LiNbO_3$ plate [21]. When ice is formed on the plate surface completely, the modified waves at 44 and 49.74 MHz are totally disappeared, while amplitude of the common wave at 53 MHz is almost the same in air, water, and ice (Fig. 10). We believe that like for common Lamb waves [21] the physical reasons of these properties are deep penetration of the modified waves into adjacent medium (glycerin, ice) enhancing attenuation of the waves because of the medium imperfections. In-plane vibration of the modified waves makes additional attenuation of the modified waves more strong.

4. Conclusions

Acoustic spectrum of plate modes in crystal plates is manifold even for a given material, orientation, plate thickness, and propagation direction. It consists of two- and three-partial Lamb waves, SH- and L-modes as well as a group of waves with elliptic polarization oriented parallel to the plate faces. In plates of ST,X-quartz the modified waves belong to high order modes ($n \geq 6$), have large velocity ($v_n > 6300$ m/s), and maintain unusual polarization at any depth from free faces for wide range of plate thickness. Do the waves exist in other crystals, what is the background of the waves, do they need piezoelectric effect and anisotropy - are not known yet. Nevertheless, it is already clear that thanks to small radiation into adjacent liquid the modified Lamb waves are promissing for sensing liquids and liquid-to-solid phase transitions as they have record sensitivity to the measurants.

Declaration of Competing Interest

The authors declare that they have no known competing financial interests or personal relationships that could have appeared to influence the work reported in this paper.

Acknowledgment

This research was funded by Russian Science Foundation, grant number # 20-19-00708.

References

[1] B.A.Auld, Acoustic Fields and Waves, Wiley, New York, 1973, vol.2, p.414.
[2] B.D. Zaitsev, I.E. Kuznetsova, S.G. Joshi, I.A. Borodina, Acoustic waves in piezoelectric plates bordered with viscous and conductive liquids, Ultrasonics 39 (2001) 45–50.
[3] A.M.Lomonosov, P.D.,Pupyrev P.Hess, Leaky Wedge Waves in Single Crystal Silicon, in: Proc. of the 2003 IEEE Ultrasonics Symposium, Prague, 21-25 July 2003, pp. 1362-1365, 2003.
[4] V. Ivan, Anisimkin, New type of an acoustic plate modes: quasi-longitudinal normal wave, Ultrasonics 42 (2004) 1095–1099.
[5] V.Yantchev, I.Katardjiev, Micromachined thin film plate acoustic resonators utilizing the lowest order symmetric Lamb wave mode, IEEE Trans. Ultrason, Ferroelect., Freq. Contr., UFFC-54 (2007) 87-95, doi: 10.1109/TUFFC.2007.214.
[6] Yu.V.Gulyaev, Peculiarities of the Anisimkin Jr.' plate modes in LiNbO3 and Te single crystals", IEEE Trans. Ultrason, Ferroelect., Freq. Contr., UFFC-56 (2009) 1042-1045.
[7] M. Onoe, S. Kaga, Analytical study of Anisimkin's (Quazilongitudinal) modes in piezoelectric plates, in: 2010 IEEE International Frequency Control Symposium, New Port Beach, California – June 2–4, 2010, paper ID 6041, 2010.
[8] W.Soluch, M.Lysakowska, Properties of shear horizontal acoustic plate modes in BT-cut quartz, IEEE Trans. Ultrason. Ferroelectr. Freq. Control, UFFC-58 (2011) 2239–2243.
[9] J. Zou, C.-M. Lin, D.G. Senesky, A. Pisano, Thermally stable SiO2/AlN/SiO2 Lamb wave resonators utilizing the lowest-order symmetric mode at high temperatures, in: 2013 Proc IEEE Ultrason. Symp., pp. 1077–1080, 2013.
[10] C. Caliendo, F. Lo Castro, Quasi-linear polarized modes in Y-rotated piezoelectric $GaPO_4$ plates, Crystals 4 (2014) 228–240.
[11] Z. Chen, L. Fan, S. Zhang, H. Zhang, Theoretical research on ultrasonic sensors based on high-order Lamb waves, J. Appl. Phys. 115 (2014) 14–20.
[12] J. Zou, A.P. Pisano, Temperature compensation of the AlN Lamb wave resonator utilizing the S1 mode, in: Proc IEEE Ultrason. Symp., 2015, pp. 07329432, 2015.
[13] Y.-F. Wang, T.-T. Wang, J.-P. Liu, Y.-S. Wang, V. Laude, Guiding and splitting Lamb waves in coupled-resonator elastic waveguides, Composite Structures 206 (2018) 588–593.
[14] V.I. Anisimkin, N.V. Voronova, Features of normal higher-order acoustic wave generation in thin piezoelectric plates, Acoust. Phys. 66 (2020) 1–4.
[15] I.E.Kuznetsova, I.A.Nedospasov, A.V.Smirnov, Z.Qian, B.Wang, X.Dai, Excitation and detection of evanescent acoustic waves in piezoelectric plates: Theoretical and 2D FEM modeling, Ultrasonics, 99 (2019). 2019. 105961, 10.1016/j.ultras.2019.105961.
[16] B.D. Zaitsev, I.E. Kuznetsova, I.A. Nedospasov, A.V. Smirnov, A.P. Semyonov, New approach to detection of guided waves with negative group velocity: Modeling and experiment, Journal of Sound and Vibration 442 (2019) 144–166, https://doi.org/10.1016/j.jsv.2018.10.056.
[17] R. Lu, Y. Yang, S. Link, S. Gong, Enabling high order Lamb wave acoustic devices with complementary oriented piezoelectric thin films, Journal of Microelectromichanical Systems 29 (2020) 1332–1346, https://doi.org/10.1109/JMEMS.2020.3007590.
[18] P. Li, L. Cheng, Propagation of shear waves in a periodically corrugated quartz crystal plate and its application exploration in acoustic wave filters, Ultrasonics 77 (2017) (2017) 100–109, https://doi.org/10.1016/j.ultras.2017.02.004.
[19] V.Yanchev, I.Katardjiev, Thin film Lamb wave resonators in frequency control and sensing applications: a review, Journal of Micromechanics and Microengineering, 23 (2013). 2013. 043001.

[20] W. Wang, Y. Yin, Y. Jia, M. Liy, Y. Kiang, Y. Zhang, M. Lu, Development of Love wave based device for sensing icing process with fast response, J. Electr/ Eng. Technol. 15 (2020) 1245–1254.
[21] V.I.Anisimkin, V.V.Kolesov, A.S.Kuznetsova, E.S.Shamsutdinova, I.E. Kuznetsova, An analysis of the water-to-ice phase transition using acoustic plate waves, Sensors, 21 (2021) 919+12 (http://doi.org/10.3390/s21030919).
[22] E.L.Adler, J.K.Slaboszewics, G.W.Farnell, and C.K.Jen, PC software for SAW propagation in anisotropic multi-layers", IEEE Trans. Ultrason., Ferroelect., Freq. Contr., UFFC-37 (1990) 215-220.
[23] A.J.Slobodnik Jr., E.D.Conway, R.T.Delmonico, Microwave Acoustic Handbook, AFCRL198 TR-73-0597, 1973.
[24] I.V.Anisimkin, V.I.Anisimkin, Attenuation of acoustic normal modes in piezoelectric plates loaded by viscous liquids, IEEE Trans.Ultrason., Ferroelect., Freq.Contr., UFFC-53 (2006)1487-1492.